

Heavy Quark Potentials in Some Renormalization Group Revised AdS/QCD Models

Ding-fang Zeng*

Institute of Theoretical physics, Beijing University of Technology

(Dated: October 22, 2018)

We construct some AdS/QCD models by the systematic procedure of GKN. These models reflect three rather different asymptotics the gauge theory beta functions approach at the infrared region, $\beta \propto -\lambda^2$, $-\lambda^3$ and $\beta \propto -\lambda$, where λ is the 't Hooft coupling constant. We then calculate the heavy quark potentials in these models by holographic methods and find that they can more consistently fit the lattice data relative to the usual models which do not include the renormalization group improving effects. But only use the lattice QCD heavy quark potentials as constrains, we cannot distinguish which kind of infrared asymptotics is the better one.

PACS numbers: 11.10.Hi, 11.25.Tq, 12.38.Aw, 12.38.Lg

I. INTRODUCTION

The Duality between string theories in Anti-deSitter space and conformal field theories on its boundary, i.e., AdS/CFT, are powerful tools for understanding the strong coupling gauge theory phenomena. In its most well known formulations, the duality is between the 4-dimensional $\mathcal{N} = 4$ super Yang-Mills field theory and type IIB super string theory in the $AdS_5 \times S_5$ background [1], [2]. In practice, our greatest interest is not $\mathcal{N} = 4$ SYM, which is conformal and non-confining, instead it is the $N_c = 3$, $N_f = 4$ or $N_f = 6$ Quantum Chromodynamics, i.e. QCD, which has running coupling and confining properties.

To obtain predictions about the practical QCD theories through AdS/CFT, or more generally, the holographic principle, people develop two ways, (i) the top-down method and (ii) the bottom-up approach. In the first method, people either construct dual string/gravity descriptions for gauge theories with running couplings, e.g. cascading gauge theories[3], or build models for gauge theories with fewer super-symmetries relative to the $\mathcal{N} = 4$ SYM[4][5]. For examples, some models implement fundamental flavors by adding probe branes in various exact or asymptotically $AdS_5 \times X_5$ background [6][7], see also [8] for reviews. The top-down method preserves fundamental structures of string theory and its dual gravity description is 10 dimensional.

In the second way, now known as AdS/QCD, people start from some 5 dimensional effective gravity theory and calculate the relevant 4D gauge theory quantities through holographic method. By requiring the results coincide with those from QCD phenomenologies, people obtain the general properties of the dual gravity background, which can be refined for further phenomenological goals. In the earliest implementation of this ideal by Polchinsky and Strassler [9], an infra-red cut off on the dual AdS_5 background is introduced to implement confinement, hence the name hard wall model. Since

the space-time of gravity descriptions ends below the cut off, appropriate boundary conditions must be imposed on this point by hand, see e.g., reference [10] and [11]. In reference [12], it is proposed that, by adding quark masses/condensates, this model can become a remarkably good model of chiral symmetry broken dynamics. Reference [13] considered a natural extension of this model by replacing the pure AdS background with a dilaton-deformed one and get very similar results. To improve the Regge behavior of highly excited rho mesons and higher spin mesons in the hard wall model, reference [14] proposed the soft wall model, where the infra-red hard wall is replaced by a dilaton quadratically depending on the holographic radial coordinate. While reference [15] and [16] proposed to include the same effects by a simple factor e^{cz^2} in front of the dual geometry's metric. Different from this guess and trial approach, in references [17], [18] and [19] GKN(Gürsoy, Kiritsis, and Nitti) propose a systematic procedure for dual geometry's construction and provide several models as illustrations.

We will introduce GKN's procedure and construct our own models in the next section. To make our dual geometries as simple as possible, so that more QCD quantities can be calculated conveniently and analytically, we do not require our models' β function to exactly coincide with the perturbative QCD theory to higher loops, like those provided in GKN's original work. The next next section discusses the calculation of heavy quark potentials in the resulting models. Numerical fittings as well as discussions about the quantum corrections are also provided in that section. The last section contains our main conclusions and prospects for future studies.

II. THE MODELS

By GKN's arguments, the non-critical string background dual to QCD like gauge theories can be described by the following Einstein frame action

$$S = \frac{1}{16\pi G_5} \int d^5x \sqrt{-G} \left[R - \frac{4}{3}(\partial\Phi)^2 + V(\Phi) \right] \quad (1)$$

*Electronic address: dfzeng@bjut.edu.cn

where we have neglected the effects of an axion field, which is of $\mathcal{O}(N_c^{-2})$ relative to the terms written out explicitly; the potential $V(\Phi)$ encodes various contributions such as the higher α' corrections and the integration of RR 4-form field whose flux seeds the $D3$ branes and $U(N_c)$ gauge group. Its functional form cannot be derived out explicitly from the first principle, but can be determined through inputs of QCD phenomenologies, e.g., the β function describing the running of coupling constant.

Setting the dual gravity geometry as

$$\Phi = \phi(u) \quad (2a)$$

$$ds^2 = e^{2A}(-dt^2 + d\vec{x} \cdot d\vec{x}) + du^2, \quad (2b)$$

and introducing phase space variable $X = \frac{\Phi'}{3A'}$, GKN find that the dilaton field's equation of motion and Einstein equations following from the action (1) can be written as first order forms,

$$\Phi' = \frac{\sqrt{3V_0}}{2} X e^{-\frac{4}{3} \int_{-\infty}^{\Phi} X d\Phi} \quad (3a)$$

$$A' = \frac{\sqrt{3V_0}}{6} e^{-\frac{4}{3} \int_{-\infty}^{\Phi} X d\Phi} \quad (3b)$$

$$V(\Phi) = V_0(1 - X^2) e^{-\frac{8}{3} \int_{-\infty}^{\Phi} X d\Phi} \quad (3c)$$

where $\Phi' = \frac{d\Phi}{du}$ and $A' = \frac{dA}{du}$. After identifying the exponentiated dilaton field with the 't Hooft coupling constant $\lambda \equiv N_c g_{YM}^2$ and the metric function $e^{A(u)}$ with the QCD energy,

$$e^{\Phi} = \lambda, \quad e^{A(u)} \propto E \quad (4)$$

GKN set up an explicit relation between the gauge theory β function and the gravity theory quantities Φ and A ,

$$\beta(\lambda) \equiv \frac{d\lambda}{d \ln E} = \lambda \frac{d\Phi}{dA} = 3\lambda X \quad (5)$$

To implement asymptotical freedom in the dual gauge theory, it is required that $A(u) \rightarrow u$, $\Phi \rightarrow -\infty$ as $u \rightarrow \infty$, i.e., the dual space-time is asymptotically anti-deSitter. Obviously, in this construction of AdS/QCD models, the non-perturbative β function determines the whole structure of the dual gravity theories. In turn, as long as we know the latter, we can use it to calculate more QCD phenomenological quantities through the holographic method.

In this paper, we will consider 3 models, each with exact (non-perturbative effects included) β function

$$\text{Model 1 : } \beta(\lambda) = -b\lambda^2 \quad (6)$$

$$\text{Model 2 : } \beta(\lambda) = -b_0\lambda^2 - b_1\lambda^3, \quad b_0, b_1 > 0 \quad (7)$$

$$\text{Model 3 : } \beta(\lambda) = -\frac{b_0\lambda^2}{1 + b_1\lambda}, \quad b_0, b_1 > 0 \quad (8)$$

respectively. At the perturbative limit, model 1 reproduces QCD's beta function to 1 loop order; model 2 reproduces the desired β function to 2 loop order; model 3

only reproduces the desired (perturbative) β function to 1 loop order. Nevertheless, there are evidences that non-perturbative effects indeed produce β functions of the model 3 type, see e.g. [20], [21] and [22]. The author of reference [22] tells us that, this kind of beta function reproduces exactly all of the known results and also the two loops. At the strong coupling limit, model 1's β function approaches infinite as $-\lambda^2$, model 2 as $-\lambda^3$, while model 3, $-\lambda$. By GKN's general confinement criteria, model 3 is critical confining, while model 1 and model 2 are super-confining.

For model 1, according to GKN's procedure,

$$\beta = -b\lambda^2 = \frac{d\lambda}{dA} \Rightarrow A = \frac{1}{b\lambda} \quad (9)$$

$$\lambda' = \lambda \Phi' = \ell^{-1} \beta e^{-\frac{4}{3} \int_{-\infty}^{\Phi} X d\Phi} = -\ell^{-1} b \lambda^2 e^{\frac{4}{3} b \lambda} \quad (10)$$

$$\Rightarrow \frac{du}{d\lambda} = (\lambda')^{-1} = -\frac{\ell e^{-\frac{4}{3} b \lambda}}{b \lambda^2}, \quad \ell \equiv \frac{6}{\sqrt{3V_0}} \quad (11)$$

so the dual gravity background can be written out explicitly

$$ds^2 = e^{2A}(-dt^2 + d\vec{x} \cdot d\vec{x}) + \ell^2 e^{2D} d\lambda^2 \quad (12)$$

$$\Phi(\lambda) = \log \lambda, \quad e^A = e^{\frac{1}{b\lambda}}, \quad e^D = \frac{e^{-\frac{4}{3} b \lambda}}{b \lambda^2} \quad (13)$$

where we use λ as the radial holographic coordinate. Using eq(3c), we know that the potential of this model's dilaton field is,

$$V(\lambda) = V_0(1 - \frac{b^2 \lambda^2}{9}) e^{\frac{8}{3} b \lambda} \quad (14)$$

From this potential, we easily see that the dual gravity background is asymptotically AdS in the ultraviolet limit but not so in the infrared region.

From equation (11), we know that

$$\int_{\infty}^u du = -\ell \int_0^{\lambda} \frac{e^{-\frac{4}{3} b \lambda}}{b \lambda^2} d\lambda \quad (15)$$

By definition and iteration formulas of the incomplete Gamma function, this leads to

$$\begin{aligned} u &= \frac{4}{9} \ell \int_{\lambda}^{\infty} \frac{e^{-\frac{4}{3} b \lambda}}{(\frac{4}{3} b \lambda)^2} d(\frac{4}{3} b \lambda) = \frac{4}{9} \ell \cdot \Gamma[-1, \frac{4}{9} b \lambda] \\ &= \frac{4}{9} \ell \cdot \left[e^{-\frac{4}{3} b \lambda} \left(\frac{4}{3} b \lambda\right)^{-1} + \Gamma[0, \frac{4}{9} b \lambda] \right] \end{aligned} \quad (16)$$

Note that $x\Gamma[0, x]_{x \rightarrow 0} \rightarrow 0$, relative to the first term, the second term on the r.h.s of (16) can be neglected. So in the ultraviolet region, $\lambda \rightarrow 0$, $u \rightarrow \frac{\ell}{b\lambda}$, $A = \frac{1}{b\lambda} \rightarrow \frac{u}{\ell}$. Using domain wall coordinates (2b), the gravity background can be easily looked out being asymptotically AdS. While in the infra-red region $\lambda \rightarrow \infty$, the scale factor of the domain wall coordinate $e^A = e^{\frac{1}{b\lambda}} \rightarrow 1$ this forms a natural softwall for the dual gravity background.

For model 2, by the same procedure as previous we know the dual gravity background and the corresponding dilaton potential are

$$\begin{aligned} \beta &= -b_0\lambda^2 - b_1\lambda^3 = \frac{d\lambda}{dA} \\ \Rightarrow ds^2 &= e^{2A}(-dt^2 + d\vec{x} \cdot d\vec{x}) + \ell^2 e^{2D} d\lambda^2 \end{aligned} \quad (17)$$

$$\begin{aligned} \Phi(\lambda) &= \log \lambda, \quad e^A = e^{\frac{1}{b_0\lambda}} \left[\frac{b_0}{b_1\lambda} + 1 \right]^{-\frac{b_1}{b_0}} \\ e^D &= \frac{e^{-\frac{4}{9}(b_0\lambda + \frac{1}{2}b_1\lambda^2)}}{b_0\lambda^2 + b_1\lambda^3}; \end{aligned} \quad (18)$$

and

$$V(\lambda) = V_0 \left[1 - \frac{1}{9}(b_0\lambda + b_1\lambda^2)^2 \right] e^{\frac{8}{9}(b_0\lambda + \frac{1}{2}b_1\lambda^2)} \quad (19)$$

respectively. Obviously, in the ultraviolet region $\lambda \rightarrow 0$, this model has the same asymptotical background — AdS space-time — as model 1. While in the infra-red region,

$$\begin{aligned} \frac{du}{d\lambda} &\rightarrow -\ell \frac{e^{-\frac{2}{9}b_1\lambda^2}}{b_1\lambda^3} \\ \Rightarrow u &= \frac{4}{9}\ell \cdot \Gamma\left[-1, \frac{2}{9}b_1\lambda^2\right] \\ &= \frac{4}{9}\ell \cdot \left[e^{-\frac{2}{9}b_1\lambda^2} \left(\frac{2}{9}b_1\lambda^2\right)^{-1} + \Gamma\left[0, \frac{2}{9}b_1\lambda^2\right] \right] \end{aligned} \quad (20)$$

So in this model, the rate of $u \rightarrow 0$ as $\lambda \rightarrow \infty$ is different from that in model 1, but the qualitative conclusions that, (i) $u \rightarrow 0$ as $\lambda \rightarrow \infty$, (ii) the dual gravity background is not asymptotically AdS in the infra-red limit, (iii) the dual gravity space-time's scale factor $e^A \xrightarrow{\lambda \rightarrow \infty} 1$ are common between the two models.

For model 3,

$$\begin{aligned} \beta &= -\frac{b_0\lambda^2}{1+b_1\lambda} = \frac{d\lambda}{dA} \\ \Rightarrow ds^2 &= e^{2A}(-dt^2 + d\vec{x} \cdot d\vec{x}) + \ell^2 e^{2D} d\lambda^2 \end{aligned} \quad (21)$$

$$\begin{aligned} \Phi(\lambda) &= \log \lambda, \quad e^A = e^{\frac{1}{b_0\lambda}} (b_0\lambda)^{-\frac{b_1}{b_0}} \\ e^D &= \frac{(1+b_1\lambda)^{1-\frac{4b_0}{9b_1}}}{b_0\lambda^2} \end{aligned} \quad (22)$$

$$V(\lambda) = V_0 \left[1 - \frac{b_0^2\lambda^2}{9(1+b_1\lambda)^2} \right] (1+b_1\lambda)^{\frac{8b_0}{9b_1}} \quad (23)$$

In the ultraviolet region, $\lambda \rightarrow 0$, $\frac{du}{d\lambda} = -e^D \rightarrow -\frac{\ell}{b_0\lambda^2}$, $u \rightarrow \frac{\ell}{b_0\lambda}$, $e^A \rightarrow e^{\frac{1}{b_0\lambda}}$. So, like the previous two models, this model also has asymptotically AdS geometry. But in the infra-red region, this model's dual space-time scale factor $e^A \rightarrow (b_0\lambda)^{-\frac{b_1}{b_0}}$ shrinks to zero as $\lambda \rightarrow \infty$, the corresponding domain wall coordinate u approaches zero as $\lambda \rightarrow \infty$ by the following law

$$u \sim \ell \frac{9b_1^2}{4b_0^2} (b_1\lambda)^{-\frac{4b_0}{9b_1}}. \quad (24)$$

In summary, all three models have the same ultraviolet asymptotic geometries — AdS space-time plus running

dilaton field. In the infrared region, the first two model's dual space-time scale factor approaches to 1 as $\lambda \rightarrow \infty$, but third model's scale factor shrinks to zero size as $\lambda \rightarrow \infty$. The domain wall coordinate u of model 1 approaches zero at the rate $u \sim 2e^{-\frac{4}{9}b\lambda}$, that of model 2 at the rate $u \sim 4e^{-\frac{2}{9}b_1\lambda^2}$, while that the model 3, $u \sim (b_1\lambda)^{-\frac{4b_0}{9b_1}}$.

III. HEAVY QUARK POTENTIALS

The heavy quark potential is an important quantity related with confinement. It is measured with high precision in lattice simulations, see reference [23] and [24]. The results are usually fit into rational polynomials

$$E(\rho) = -\frac{\kappa}{\rho} + \frac{\kappa'}{\rho^2} + \frac{\rho}{a^2} + C \quad (25)$$

where ρ is the distance between the quark and anti-quark while κ , κ' and a^2 are parameters to be determined by fittings, C is an irrelevant normalizing constant. In gauge theories, this potential is related to the expectation value of rectangular Wilson loops of width ρ and length T

$$\langle W \rangle = \exp[-E(\rho)T] \quad (26)$$

here T can be understood as the time the quark and anti-quark are bounded together. By the gauge/string duality conjectures, $\langle W \rangle$ equates to the partition function of an open string which is living on the AdS background and whose world sheet boundary coincides with the Wilson loop

$$\langle W \rangle = \exp[-E(\rho)T] \sim Z = \int \mathcal{D}X^\mu \exp(-S) \quad (27)$$

where S is the Nambu-Goto action of the string. Let $x^\mu(\sigma, \tau)$ denote the classical string profile and ξ^μ the quantum fluctuation around it. Obviously, the path integral will be dominated by the classical string configuration since it minimizes S , this means

$$\begin{aligned} Z &= \exp(-S_c[x]) \int \mathcal{D}\xi \exp[-S(x+\xi) + S_c(x)] \\ &\approx \exp(-S_c[x]) \int \mathcal{D}\xi \exp[-\xi^{a\dagger} \mathcal{O}_a \xi^a] \end{aligned} \quad (28)$$

So in the classical approximation, the heavy quark potentials read

$$E(\rho)T \approx S_c[x] \quad (29)$$

While to first order quantum corrections

$$E(\rho)T \approx S_c[x] - \sum \log \det \mathcal{O}_a \quad (30)$$

In the following, we will calculate the heavy quark potentials quantitatively in the classical approximations and study the quantum corrections qualitatively. We do not get quantitative results on the latter. But even in the classical approximation level, the models provided in this paper predict heavy quark potentials more consistently fitting with the lattice QCD results than almost all the models considered in [28].

A. Classical Approximations

In the classical approximations, to have the given Wilson loop as the world sheet boundary, the string must have its two ends fixed on the boundary and the center part dips into the bulks of the background AdS space-time

$$x^0 = \tau, \quad x^1 = \sigma, \quad \lambda = \lambda(\sigma), \quad x^{2,3} \text{ fixed} \quad (31a)$$

$$\sigma \in \left[-\frac{\rho}{2}, \frac{\rho}{2}\right] \quad (31b)$$

$$\lambda\left(-\frac{\rho}{2}\right) = \lambda\left(\frac{\rho}{2}\right) = 0, \quad \lambda(0) = \lambda_0 \quad (31c)$$

For this configuration, the classical Nambu-Goto action can be written as $S_c = E_c \cdot \int d\tau$, with

$$E_c = \frac{1}{\pi\alpha'} \int_0^{\frac{\rho}{2}} d\sigma \sqrt{e^{\frac{8\Phi}{3}} e^{2A} (e^{2A} + \ell^2 e^{2D} \lambda_{,\sigma}^2)} \quad (32)$$

where $\lambda_{,\sigma}$ denotes $\frac{d\lambda}{d\sigma}$. Since the classical configuration minimizes S_c we know

$$\frac{e^{\frac{8\Phi}{3}} e^{4A}}{\sqrt{e^{\frac{8\Phi}{3}} e^{2A} (e^{2A} + \ell^2 e^{2D} \lambda_{,\sigma}^2)}} = \text{const.} = e^{\frac{4}{3}\Phi_0} e^{2A_0} \quad (33)$$

$$\Rightarrow \ell \lambda_{,\sigma} = \pm e^{A-D} \sqrt{e^{\frac{8}{3}\Phi} e^{4\tilde{A}} - 1} \quad (34)$$

in the above derivation, we have used the fact that at the center point of the string $\sigma = 0$, $\lambda_{,\sigma} = 0$. Using eqs(33) and (34), both the distance ρ between the two ends of the string and its energy E_c can be expressed as functions of λ_0 .

$$\rho = 2\ell e^{-A_0} \int_0^{\lambda_0} d\lambda \frac{e^{D-3\tilde{A}} \tilde{\lambda}^{-\frac{4}{3}}}{\sqrt{1 - \tilde{\lambda}^{-\frac{8}{3}} e^{-4\tilde{A}}}} \quad (35)$$

$$E_c = \frac{\ell \lambda_0^{\frac{4}{3}} e^{A_0}}{\pi\alpha'} \int_0^{\lambda_0} d\lambda \frac{\tilde{\lambda}^{\frac{4}{3}} e^{D+\tilde{A}}}{\sqrt{1 - \tilde{\lambda}^{-\frac{8}{3}} e^{-4\tilde{A}}}} \quad (36)$$

where $\tilde{A} \equiv A - A_0$ while $\tilde{\lambda} = \frac{\lambda}{\lambda_0}$. Since the string is infinitely long, the total energy in (36) is divergent. In the Gauge theory side, this means that quark-antiquark pairs are infinitely heavy. To obtain the finite interaction energy, we will subtract from E_c the infinite rest mass part, which corresponds to that of two straight strings, see reference [25] and [26]. Taking model 1 as an example, this means

$$E_{c,q\bar{q}} = \frac{\ell \lambda_0^{\frac{4}{3}} e^{A_0}}{\pi\alpha'} \left[\int_0^{\lambda_0} d\lambda \frac{\tilde{\lambda}^{\frac{4}{3}} e^{D+\tilde{A}} [1 - \sqrt{\dots}]}{\sqrt{1 - \tilde{\lambda}^{-\frac{8}{3}} e^{-4(\tilde{\lambda}^{-1}-1)/c}}} - \int_{\lambda_0}^{\infty} d\lambda \tilde{\lambda}^{\frac{4}{3}} e^{D+\tilde{A}} \right] \quad (37)$$

where $\tilde{\lambda} \equiv \frac{\lambda}{\lambda_0}$, $c \equiv b\lambda_0$ and the ' $\sqrt{\dots}$ ' still means an expression the same as the denominator. To assure the integrand of the right hand side take real values in the range

$\tilde{\lambda} \in [0, 1]$, the parameter c must be less than $\frac{3}{2}$. Through qualitative analysis of, we know that ρ is a monotonically increasing function of c .

Under the long separation limit which corresponds to $c \rightarrow \frac{3}{2}$, the potentials can be calculated easily

$$\begin{aligned} E_{c,q\bar{q},\rho \rightarrow \infty} &\stackrel{c \rightarrow \frac{3}{2}}{\approx} \frac{\lambda_0^{\frac{4}{3}} e^{2A_0}}{2\pi\alpha'} \cdot \rho + \frac{\ell \lambda_0^{\frac{4}{3}} e^{A_0}}{\pi\alpha'} \int_{\lambda_0}^{\infty} d\lambda \tilde{\lambda}^{\frac{4}{3}} e^{D+\tilde{A}} \\ &= \frac{\lambda_0^{\frac{4}{3}} e^{2A_0}}{2\pi\alpha'} \cdot \rho + \frac{\ell \left(\frac{3}{2}\right)^{\frac{2}{3}} e^{\frac{1}{c}}}{\pi\alpha' b^{\frac{4}{3}}} \Gamma\left[\frac{1}{3}, \frac{4c}{9}\right]_{c \rightarrow \frac{3}{2}} \end{aligned} \quad (38)$$

While at the short separation limit $c \rightarrow 0$.

$$\rho \stackrel{c \rightarrow 0}{\approx} 2\ell e^{-\frac{1}{c}} (0.596 + 0.0471c + \mathcal{O}[c^2]) \quad (39)$$

$$E_{c,q\bar{q}} \stackrel{c \rightarrow 0}{\approx} \frac{2\ell c^{\frac{4}{3}} e^{\frac{1}{c}}}{\pi\alpha' b^{\frac{4}{3}}} (-0.602 + 0.042c + \mathcal{O}[c^2]) \quad (40)$$

Which means that

$$\begin{aligned} E_{c,q\bar{q},\rho \rightarrow 0} &= -\frac{2\ell^2}{\pi\alpha' b^{4/3}} \frac{\epsilon(c)|_{c=c(\rho)}}{\rho} \\ \epsilon(c) &= c^{4/3} [0.359 + 0.003c + \dots] \end{aligned} \quad (41)$$

the functional form of $c(\rho)$ should be obtained by reversing the relation (39). For example, to first order approximation in $[\log \frac{\ell}{\rho}]^{-1}$, we can use iteration method to obtain

$$c \approx \left(\log \left[\frac{1.19\ell}{\rho} + \frac{0.0942\ell}{\rho} \left(\log \frac{1.19\ell}{\rho} \right)^{-1} \right] \right)^{-1} \quad (42)$$

Since the series expression for $\rho(c)$ in eq(39) is incomplete, its inverse (42) is not well-defined as $\rho > 1.19\ell$. We assume that $c(\rho)_{\rho > 0.8/\text{Gev}} \equiv c(0.8/\text{Gev})$. Combining eqs(38) and (41) together, the classically approximated heavy quark potential of model 1 can be written as follows

$$\begin{aligned} E_{c,q\bar{q}}(\rho) &= -\frac{2\ell^2}{\pi\alpha' b^{4/3}} \frac{\epsilon(c)_{c=c(\rho)}}{\rho} + \frac{\left(\frac{3}{2}\right)^{\frac{4}{3}} e^{\frac{4}{3}}}{2\pi\alpha' b^{\frac{4}{3}}} \rho \\ &\quad - \frac{\left(\frac{3}{2}\right)^{\frac{2}{3}} e^{\frac{2}{3}} \ell}{\pi\alpha' b^{\frac{4}{3}}} \Gamma\left[\frac{1}{3}, \frac{2}{3}\right] \end{aligned} \quad (43)$$

Figure 1 compares this result with the direct numerical integrations intuitively. From the figure we see that the analytical formula captures the main properties of the integration remarkably well. For model 2 and model 3, the potentials can be calculated similarly, and the results are also similar. But the precision of the analytical approximation is lower than model 1. For this reason, in the following fittings, we use numerics to get the $\rho - E_{c,q\bar{q}}$ relations for all the three models directly.

Eq(43) does not have the standard Cornell potential form, for its $\frac{1}{\rho}$ term(or the Luscher term) has a ρ -dependent coefficient, which is proportional to

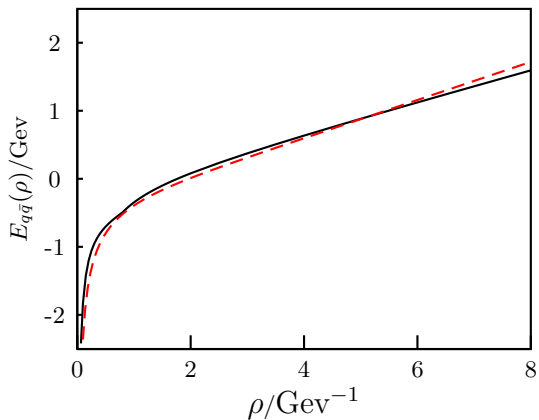


FIG. 1: Heavy quark potentials in model 1, the continuous line is the result of analytical approximation (43), while the dashed line comes from direct numerical integration of eq(35) and (37).

$[\log \frac{1.19\ell}{\rho}]^{-\frac{4}{3}}$. This is determined by asymptotical behavior¹ of the beta function $\beta \propto -\lambda^2$ and is a common prediction of all the renormalization group revised models constructed by GKN's general procedure [18], [19]. Just as we will show in the following, this feature makes these models predict $\rho - E_{q\bar{q}}$ relations more consistently fitting with the lattice data than those which do not include the renormalization effects.

B. Comparing with lattice results

Figure 2 compares the the heavy quark potentials following from our AdS/QCD models and those of lattice results. The relevant parameters are listed in table I and are fixed by fits, which is required to minimize the following χ^2 variable

$$\chi^2 = \sum_{i=1}^{N_{data}} \frac{(E_i^{AdS/QCD} - E_i^{latt.})^2}{\sigma_i^2} \quad (46)$$

where the sum is over all the used data points and σ_i is the absolute error of the i th point. From the figure we see that almost all the three models fit with the lattice data equally well. This means that in the AdS/QCD framework, only by fitting with lattice data on heavy quark potentials, we cannot distinct the infrared behavior of the gauge theory β function.

¹ If we assume that

$$\beta \rightarrow -b\lambda^p, \quad p > 1 \quad (44)$$

then, by the same calculations as above, we will find that

$$E_{q\bar{q},\rho \rightarrow} = -\frac{[\log \frac{1.19\ell}{\rho}]^{-\frac{4}{3(p-1)}}}{\rho} + \text{other terms} \quad (45)$$

	ρ_{cut}	parameters	Best fit
Model 1	1.0	$\alpha' b_0^{\frac{4}{3}}$	4.99
		ℓ	4.71
		const	-0.013
Model 2	1.0	$\alpha' b_0^{\frac{4}{3}}$	4.38
		ℓ	4.37
		b_1/b_0^2	0.011
		const	0.018
Model 3	1.0	$\alpha' b_0^{\frac{4}{3}}$	4.55
		ℓ	4.25
		b_1/b_0	0.058
		const	-0.029

TABLE I: Best fit values for the parameters involved in our AdS/QCD models. All dimensional parameters use Gev⁻¹ as units.

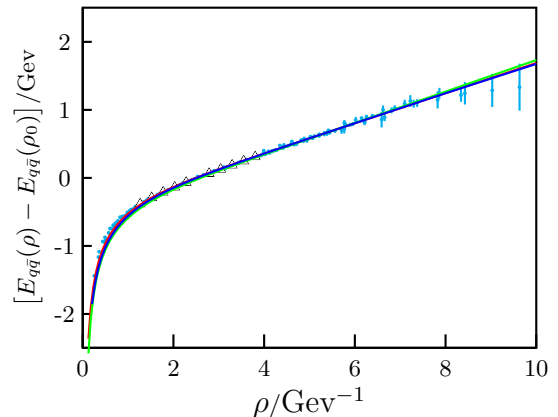


FIG. 2: Potentials $E_{q\bar{q}}(\rho)$ predicted by our AdS/QCD models. The discrete data points comes from the lattice results of quenched QCD, reference [31]. Since the three models almost fit the lattice data equally well, the three lines coincide.

Taking our FIG. 2 and the Fig.1 of reference [28] as a comparison, we easily see that our models can be more consistently fitted with the lattice data than almost all the previous models which do not include the renormalization group improvements. To make this point more clearly, we display the $\chi^2/N_{d.o.f} - \rho_{cut}$ in figure 3. Our ρ_{cut} has the same meaning as that of reference [28], which is the length scale below which the lattice data is not used to make fits. This is a manufacturing selection. Our models can give very low $\chi^2/N_{d.o.f}$ even when the ρ_{cut} is set as low as 1Gev⁻¹, while most of the AdS/QCD models which do not include the renormalization group effects can only do so when ρ_{cut} is set as 4 - 5Gev⁻¹. In another word, to make a good fit, the usual models must cut more than one half of the lattice data points while our models almost need no cut at all.

This is a really exciting result and it can be attributed to the fact that our models predict heavy quark potentials which at the short separation limit behaves like $E_{q\bar{q},\rho \rightarrow 0} \rightarrow -[\ln \frac{1.19\ell}{\rho}]^{-\frac{4}{3}}/\rho$. Considering the fact that al-

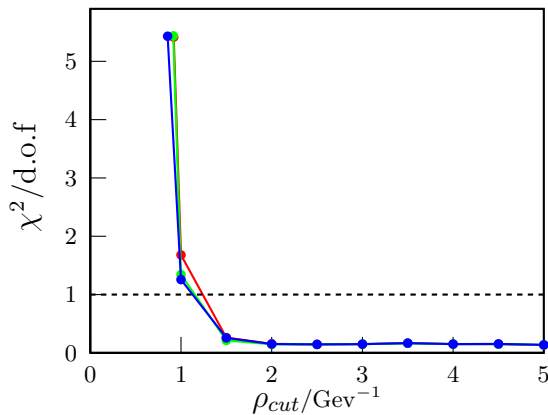


FIG. 3: Variation of the minimal $\chi^2/N_{d.o.f}$ with respect to ρ_{cut} . The red, green and blue lines are the results for our model 1, model 2 and model 3 respectively.

most all the AdS/QCD models which do not include the renormalization group effects predict $E_{q\bar{q}, \rho \rightarrow 0} \rightarrow 1/\rho$ and the quantum corrections do not change it remarkably[26], a natural question arises, will the quantum corrections in our models change the short separation limit of our potentials remarkably? We change in the following to the quantum corrections of the heavy quark potentials.

C. Quadratic quantum corrections

Including quantum corrections, to first first order approximation, the heavy quark potentials can be read out from eqs(28) and (30),

$$E(\rho)T = S_c[x] - \sum_a \log(\det \mathcal{O}_a) \quad (47)$$

To get quantitative results, we need to run 3 steps [26]. (i) choose an appropriate gauge and define the fluctuations properly, (ii) work out the corresponding action $S[x_c + \xi] - S[x_c]$ describing the fluctuations and read out from it the relevant second order differential operators \mathcal{O}_a , (iii) calculate eigenvalues of these operators and use some regularization procedures to calculate the functional determinants of them and finally extract the resulting corrections to the potential.

We will consider the fluctuations in the fixed λ — fix it on the classical profile — gauge. In this gauge the fluctuating quantities are ξ and η , whose boundary properties and relations to the complete embedding functions X^μ are

$$\begin{aligned} X^0 &= \tau, X^1 = \sigma + \xi(\tau, \sigma), \quad \lambda = \lambda(\sigma) \\ X^{2,3} &= \eta^{2,3}(\tau, \sigma) \end{aligned} \quad (48a)$$

$$\xi(\tau, \sigma)_{\tau=0, T} = 0, \quad \xi(\tau, \sigma)_{\sigma=0, \pm\rho/2} = 0 \quad (48b)$$

$$\eta(\tau, \sigma)_{\tau=0, T} = 0, \quad \eta(\tau, \sigma)_{\sigma=0, \pm\rho/2} = 0 \quad (48c)$$

where $\lambda(\sigma)$ describes the classical string profile which satisfies eq(34). Substituting these embeddings into eq(28)

and extract terms quadratic in quantities ξ and η , we have

$$\begin{aligned} S_{(2)} &= \frac{1}{2} [G_{tt}^s (G_{xx}^s + G_{\lambda\lambda}^s \lambda'^2)]^{-\frac{1}{2}} \left[G_{\lambda\lambda}^s G_{xx}^s \lambda'^2 \xi^2 + \right. \\ &\quad \left. G_{tt}^s G_{xx}^s \xi'^2 + G_{yy}^s (G_{xx}^s + G_{\lambda\lambda}^s \lambda'^2) \eta^2 + G_{tt}^s G_{yy}^s \eta'^2 \right] \end{aligned} \quad (49)$$

where the over-dots denote derivatives with respect to τ and primes denote derivatives with respect to σ . After integrating by parts and simplifying by the classical e.o.m (33), $S_{(2)}$ can be written in the form $\xi^\dagger \mathcal{O}_\xi \xi + \eta^\dagger \mathcal{O}_\eta \eta$, with

$$\mathcal{O}_\xi = -(\lambda_0^{\frac{4}{3}} e^{2A_0}) \left[\frac{1}{\rho^2} \partial_{\tilde{x}}^2 + (\tilde{\lambda}^{\frac{8}{3}} e^{4\tilde{A}} - 1) \partial_t^2 \right] \quad (50)$$

$$\mathcal{O}_\eta = -(\lambda_0^{\frac{4}{3}} e^{2A_0}) \left[\frac{1}{\rho^2} \partial_{\tilde{x}}^2 + \tilde{\lambda}^{\frac{8}{3}} e^{4\tilde{A}} \partial_t^2 \right] \quad (51)$$

where \tilde{x} is the normalized $x = \tilde{x} \cdot \rho$, this means that as x varies in the range $0 < x < \rho$, \tilde{x} varies in the range $0 < \tilde{x} < 1$. Note that η is a two component vector and η^2 actually means $\eta^{(2)} \eta^{(2)} + \eta^{(3)} \eta^{(3)}$, and similarly $\eta'^2 = \eta^{(2)'} \eta^{(2)'} + \eta^{(3)'} \eta^{(3)'}$.

Reference [26] proved that, for any operator of the form

$$\mathcal{O}[A, B] = B^2 \mathcal{O}_v + A^2 F_t(v) \partial_t^2 \quad (52)$$

if the parameter A, B encode all the dependences on the inter-quark distance ρ , while v, F_t and \mathcal{O}_v are variables or operators independent of ρ , then the functional determinant of $\mathcal{O}[A, B]$ must be of the form

$$\log(\det \mathcal{O}[A, B]) = \frac{BT}{A} \log(\det \mathcal{O}[1, 1]) + o(T) \quad (53)$$

i.e. ρ dependence of the log det of such operators is completely contained in the coefficient $\frac{B}{A}$. For almost all the models considered by [26], say the typical AdS_5/CFT_4 case, this leads to that the quadratic quantum correction to the heavy quark potentials are proportional to ρ^{-1} . However, in the current case, if we write the operators of eqs(50) and (51) into the form of eq(52), then the quantity $F_t(v) \equiv \tilde{\lambda}^{\frac{8}{3}} e^{4\tilde{A}}$ appearing in them will depend on the interquark distance implicitly, see figure 4 for details.

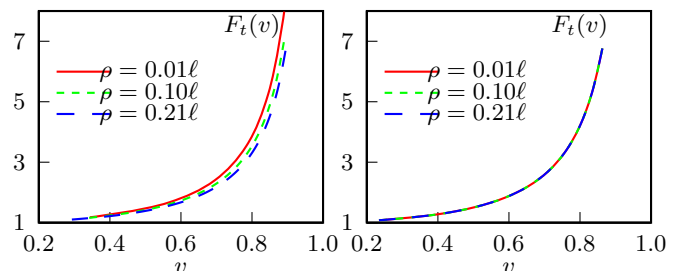


FIG. 4: Left, the function $F_t(v)$ appearing in the \mathcal{O}_η operator of eqs(51)(write it into the form of (52)), the function depends on the interquark distance ρ . Right, $F_t(v)$ for the simple AdS_5/CFT_4 correspondence, the function is independent of the interquark distance ρ

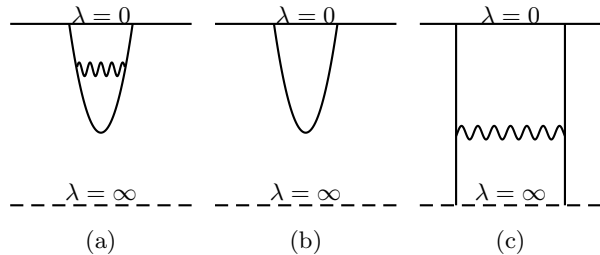


FIG. 5: String configurations contributing to the Wilson loop correlator. The upper lines denote the boundary of the asymptotically AdS space, while the lower dashed lines denote its center point. According to reference [27], figure b) is the dominant contributor to the Wilson-Polyakov loop correlators at the short separation limit; figure c) is the dominator at the long separation limit; figure a) displays quantum corrections due to the graviton-dilaton exchange process.

This is both a good and a bad news for us. The good news is, it means that we can almost definitely conclude that the quantum corrections to the heavy quark potentials is not of the $1/\rho$ type. The bad news is, it means we cannot derive out explicit functional forms for the ρ -dependence of the quadratic quantum corrections through this simple method. To get quantitative results, we need to find out the eigenvalue spectrum of \mathcal{O}_ξ and \mathcal{O}_η and their functional determinant by numerics. Since they cannot be find out analytically, the regularization of the resulting functional determinant becomes a big problem. At this point, we have no good method to overcome this obstacle numerically.

Reference [27] studied the Wilson-Polyakov loop correlators in the finite temperature $\mathcal{N} = 4$ SYM plasmas, from which the relevant heavy quark potentials can be extracted conveniently. They pointed out that although at the short separation limit, the heavy quark potentials is dominated by smooth the string configuration which minimizes the classical Nambu-Goto action, part(c) of FIG5, at the long separation limit, the potentials is dominated by string profiles which involves the exchange of the lightest graviton-dilaton modes, see the part(c) of FIG.5. According to this results, our above considerations of the quantum fluctuations(around the classical string profile) correction is not the only contribution to the interquark-potentials. We should also consider diagrams of the form like the part(a) of FIG.5. But this kind of string profile contributing to the heavy quark potentials always carries a factor of λ^2 relative to the classical profile does, and to make the area of the string world sheet as small as possible, the string cannot not fall very deep into the bulk of the space-time, i.e. they are mainly around the $\lambda \rightarrow 0$ region. So there is no need to worry that this kind of correction will change the short separation limit of our potentials.

IV. CONCLUSIONS

From the previous section, we know that the heavy quark potentials following from all our three models asymptote to the same form $E_{q\bar{q}} \propto -1/(\rho[\log \frac{1-19\ell}{\rho}]^{4/3})$ at the short separation limit. This is determined by the UV property of the gauge theory beta function $\beta \propto -\lambda^2$ and is a common feature for all the renormalization group improved AdS/QCD models constructed by GKN's procedure. Although this is different from the usual Cornell potential, through numerical fittings and comparison with reference [28], we know that our models can more consistently fit the lattice data, relative to almost all the previous AdS/QCD models which do not include the renormalization group effects, for example, those of [14], [15] and [29].

Numerical results also tells us that, though we can construct AdS/QCD models with very different infrared β function, for example $\beta \rightarrow -\lambda^2, -\lambda, -\lambda^3$, only by comparison with the lattice QCD heavy quark potentials, we cannot distinguish which one is the better. Since at long separation limit we neglected the graviton-dilaton exchange contributions to the heavy quark potentials, we should be more careful on this conclusion. Just as reference [19] showed and our numerics indicated, neglecting the graviton-dilaton exchange contributions does not affect the qualitative conclusion that the potentials following from our AdS/QCD models are linearly confined. (Reference [27] pointed out that there is many uncertainties on the quantitative calculation of the graviton-dilaton exchange contributions at the long separation limit) Nevertheless, further studies on this point and comparison with both the lattice data and the heavy quark effective field theories [32] will be interesting topics.

The above content consists the main conclusions of this paper. On the model building part, we have no unexpected conclusions. A little summary can be given as follows. Three AdS/QCD models are built by the systematic procedure of GKN. At the perturbative limit, the first model has gauge theory β function coincide with the usual QCD to 1 loop order; model 2's β function coincides with the desiring to 2 loops; while model 3, only reproduces the desiring to 1 loop order. Nevertheless, due to non-perturbative effects, the β function of model 3 may be the one most closely related to the real QCD theory. At the strong coupling limit, model 1's β function approaches infinite as $-\lambda^2$, model 2 as $-\lambda^3$, while model 3, $-\lambda$. By GKN's general confinement criteria, model 1 and model 2 are super-confining, while model 3 is critically confining. In the ultraviolet limit, the three models' dual gravity description have the same asymptotical background — AdS space-time plus running dilaton field. In the infrared region, model 1 and 2's dual space-time scale factor approaches to 1 as $\lambda \rightarrow \infty$, but model 3's scale factor shrinks to zero size as $\lambda \rightarrow \infty$.

For future directions, we think looking for finite tem-

perature solutions to these models and the relevant phenomenological applications of them may be interesting subjects, see e.g. references [33] [34] [35] [36] [37] [38] [39]. We hope to come back on this point in the near future.

Acknowledgements

We thank very much to professor G. S. Bali and C. D. White for reminding us their work, especially the former for explaining the lattice data related questions, including the normalization and obtaining conditions.

APPENDIX

APPENDIX A: INCOMPLETE GAMMA FUNCTION

This appendix collects some basic formulas of the incomplete Gamma function which is needed in the analytical derivation of the short separation limit of the heavy quark potentials. The content is based on the help document of software *Mathematica* and some simple variable replacements and derivations.

The incomplete Gamma function $\Gamma[a, z]$ is defined as

$$\Gamma[a, z] = \int_z^\infty t^{a-1} e^{-t} dt \quad (\text{A.1})$$

When $a > 0$, we have the following expansion formulae,

$$\Gamma[a, z] \stackrel{z \rightarrow \infty}{\simeq} e^{-z} z^{a-1} \left(1 + \frac{a-1}{z} + \frac{a^2 - 3a + 2}{z^2} + \mathcal{O}\left(\frac{1}{z}\right)^3 \right) \quad (\text{A.2})$$

$$\Gamma[a, z] \stackrel{z \rightarrow 0}{\simeq} \Gamma[a] + z^a \left(-\frac{1}{a} + \frac{z}{1+a} - \frac{z^2}{2(2+a)} + \mathcal{O}(z^3) \right) \quad (\text{A.3})$$

When $a < 0$, by definition, we can easily prove the following iteration formula,

$$\begin{aligned} \Gamma[a, z] &\stackrel{a \leq 0}{\simeq} -\frac{e^{-z} z^a}{a} + \frac{1}{a} \Gamma[a+1, z] \\ &= -\frac{e^{-z} z^a}{a} - \frac{e^{-z} z^{a+1}}{a(a+1)} + \frac{1}{a(a+1)} \Gamma[a+2, z] \end{aligned} \quad (\text{A.4})$$

For integrations like $\int_0^1 \lambda^{-p} e^{-\frac{\lambda}{c\lambda}} d\lambda$, we can translate it into incomplete Gamma functions through variable replacements

$$\int_0^1 \lambda^{-p} e^{-\frac{\lambda}{c\lambda}} d\lambda = \int_1^\infty \hat{\lambda}^{p-2} e^{-\frac{\hat{\lambda}}{c}} d\hat{\lambda} = c^{p-1} \Gamma\left[p-1, \frac{1}{c}\right] \quad (\text{A.5})$$

$$\begin{aligned} \int_\epsilon^1 \lambda^{-p} e^{-\frac{\lambda}{c\lambda}} d\lambda &= \int_1^{\frac{1}{\epsilon}} \hat{\lambda}^{p-2} e^{-\frac{\hat{\lambda}}{c}} d\hat{\lambda} \\ &= c^{p-1} \Gamma\left[p-1, \frac{1}{c}\right] - c^{p-1} \Gamma\left[p-1, \frac{1}{c\epsilon}\right] \end{aligned} \quad (\text{A.6})$$

-
- [1] J. M. Maldacena, *Adv. Theor. Math. Phys.* **2** (1998) 231–252, [hep-th/9711200](#).
- [2] S. S. Gubser, I. R. Klebanov, and A. M. Polyakov, *Phys. Lett.* **B428** (1998) 105–114, [hep-th/9802109](#); E. Witten, *Adv. Theor. Math. Phys.* **2** (1998) 253–291, [hep-th/9802150](#); *Adv. Theor. Math. Phys.* **2** (1998) 505–532, [hep-th/9803131](#).
- [3] I. R. Klebanov, Edward Witten, *Nucl. Phys.* **B536** (1998) 199–218, [hep-th/9807080](#); I. R. Klebanov, N. A. Nekrasov, *Nucl. Phys.* **B574** (2000) 263, [hep-th/9911096](#); I. R. Klebanov, A. A. Tseytlin, *Nucl. Phys.* **B578** (2000) 123, [hep-th/0002159](#); I. R. Klebanov, M. J. Strassler, *JHEP* **0008** (2000) 052, [hep-th/0007191](#).
- [4] L. Girardello, M. Petrini, M. Porrati and A. Zaffaroni, *Nucl. Phys. B* **569**, 451 (2000), [9909047v2\[hep-th\]](#); L. Girardello, M. Petrini, M. Porrati and A. Zaffaroni, *JHEP* **9905**, 026 (1999), [hep-th/9903026](#); L. Girardello, M. Petrini, M. Porrati and A. Zaffaroni, *JHEP* **9812**, 022 (1998), [9810126\[hep-th\]](#); D. Z. Freedman, S. S. Gubser, K. Pilch and N. P. Warner, *Adv. Theor. Math. Phys.* **3**, 363 (1999), [9904017v3](#); D. Z. Freedman, S. S. Gubser, K. Pilch and N. P. Warner, *JHEP* **0007**, 038 (2000), [hep-th/9906194](#); J. Polchinski and M. J. Strassler, [0003136v2\[hep-th\]](#); J. Babington, D. E. Crooks and N. J. Evans, *Phys. Rev. D* **67**, 066007 (2003), [0210068\[hep-th\]](#); N. R. Constable, R. C. Myers, *JHEP* **9911**, 020 (1999), [9905081v4](#); J. Babington, D. E. Crooks and N. J. Evans, *JHEP* **0302**, 024 (2003), [0207076\[hep-th\]](#).
- [5] T. Sakai, S. Sugimoto, *Prog. Theor. Phys.* **113** (2005) 843–882, [hep-th/0412141v5](#); *Prog. Theor. Phys.* **114**:1083–1118 [hep-th/0507073v4](#).

- [6] A. Karch, E. Katz, *JHEP* **0206** (2002) 043, hep-th/0205236; D. Arean, D. E. Crooks, A. V. Ramallo, *JHEP* **0411** (2004) 035, hep-th/0408210; P. Ouyang, *Nucl. Phys.* **B699** (2004) 207, hep-th/0311084; T. S. Levi and P. Ouyang, hep-th/0506021; T. Sakai, J. Sonnenschein, *JHEP* **0309** (2003) 047, hep-th/0305049; S. Kuperstein, *JHEP* **0503** (2005) 014, hep-th/0411097; B. A. Burrington, J. T. Liu, L. A. Pando Zayas and D. Vaman, *JHEP* **0502** (2005) 022 hep-th/0406207; B. A. Burrington, V. S. Kaplunovsky and J. Sonnenschein, 708.1234[hep-th]; R. Apreda, J. Erdmenger, D. Lust and C. Sieg, *JHEP* **0701** (2007) 079 hep-th/0610276; C. Sieg, *JHEP* **0708** (2007) 031 0704.3544[hep-th].
- [7] R. Casero, C. Nunez and A. Paredes, Phys. Rev. D73: 086005,2006, e-Print: hep-th/0602027; E. Caceres, R. Flauger, M. Ihl and T. Wrase, JHEP 0803:020,2008, e-Print: arXiv:0711.4878; F. Benini, F. Canoura, S. Cremonesi, C. Nunez, A. V. Ramallo, JHEP 0709:109,2007, e-Print: arXiv:0706.1238
- [8] J. Erdmenger, N. Evans, I. Kirsch, E. Threlfall, 0711.4467 [hep-th].
- [9] J. Polchinski, M. J. Strassler, Phys. Rev. Lett. 88 (2002) 031601, hep-th/0109174v1.
- [10] S. J. Brodsky, G. F. de Teramond, Phys. Rev. Lett. 96 : 201601 (2006), hep-ph/0602252; A. Krikun, 0801.4215 [hep-th]
- [11] L. D. Rold, A. Pomarol, Nucl. Phys. B721 (2005) 79-97, hep-ph/0501218 hep-th/0702205v1.
- [12] J. Erlich, E. Katz, D. T. Son, M. A. Stephanov, Phys. Rev. Lett. 95 (2005) 261602, hep-ph/0501128.
- [13] K. Ghoroku, N. Maru, M. Tachibana and M. Yahiro, Phys. Lett. B **633**, 602 (2006), [arXiv:hep-ph/0510334].
- [14] A. Karch, E. Katz, D. T. Son, M. A. Stephanov, Phys. Rev. D74: 015005, 2006, hep-ph/0602229v2.
- [15] O. Andreev, V. I. Zakharov, Phys. Rev. D73 : 107901, 2006 hep-th/0603170; Phys.Rev. D74 (2006) 025023, hep-ph/0604204.
- [16] E. Shuryak, hep-th/0605219v1.
- [17] F. Bigazzi, R. Casero, A. L. Cotrone, E. Kiritsis, A. Paredes, JHEP 0510 (2005) 012, hep-th/0505140.
- [18] U. Gürsoy and E. Kiritsis, eprint: 0707.1324.
- [19] U. Gürsoy, E. Kiritsis and F. Nitti eprint: 0707.1349.
- [20] P. Boucaud, F. De Soto, A. Le Yaouanc, J.P. Leroy, J. Micheli, H. Moutarde, O. Pene, J. Rodriguez-Quintero, JHEP 0304(2003)005, hep-th/0212192.
- [21] M. Frasca, e-Print arXiv: 0802.1183.
- [22] T. A. Rytlov, F. Sannino, arXiv: 0711.3745
- [23] G. S. Bali, Phys. Rept. 343 : 1-136 (2001), hep-ph/0001312.
- [24] E. Eichten, K. Gottfried, T. Konoshita, K. D. Lane and T. -M. Yan, Phys. Rev. D17 (1978) 3090, D21 (1980) 203.
- [25] J. M. Maldacena, Phys. Rev. Lett. 80, 4859 (1998), hep-th/9803002; S. J. Rey and J. T. Yee, Eur. Phys. J. C22, 379 (2001), hep-th/9803001v3.
- [26] Y. Kinar, E. Schreiber, J. Sonnenschein, Nucl. Phys. B566 (2000) 103-125, 9811192; Y. Kinar, E. Schreiber, J. Sonnenschein, N. Weiss, Nucl. Phys. B583 : 76-104(2000), hep-th/9911123v2.
- [27] D. Bak, A. Karch and L. G. Yaffe, e-Print: arXiv:0705.0994.
- [28] C. D. White, Phys. Lett. B652 : 79-85, 2007, e-Print: hep-ph/0701157.
- [29] J. P. Shock, F. Wu, Y. -L. Wu, Zh. -F. Xie, JHEP 0703:064,2007. e-Print: hep-ph/0611227.
- [30] S. Weinberg, Cambridge University Press, 1996.
- [31] G. S. Bali and K. Schilling, Phys. Rev. D47: 661-672, 1993, e-Print: hep-lat/9208028; G. S. Bali, K. Schilling and A. Wachter, Phys. Rev. D56: 2566-2589, 1997, e-Print: hep-lat/9703019; S. Necco and R. Sommer, Nucl. Phys. B622: 328-346, 2002, e-Print: hep-lat/0108008.
- [32] N. Brambilla, A. Pineda, J. Soto and A. Vairo, Rev. Mod. Phys. 77: 1423,2005, e-Print: hep-ph/0410047; N. Brambilla, J. Ghiglieri, A. Vairo and P. Petreczky, e-Print: arXiv:0804.0993. By Quarkonium Working Group (N. Brambilla et al.), Published as CERN Yellow Report, e-Print: hep-ph/0412158.
- [33] C. P. Herzog, Phys. Rev. Lett. 98:091601,2007. hep-th/0608151
- [34] Phys. Lett. B645 (2007) 437-441, hep-ph/0607026.
- [35] E. Nakano, S. Teraguchi, W.-y. Wen, Phys. Rev. D75: 085016,2007. hep-ph/0608274.
- [36] U. Gürsoy, E. Kiritsis, L. Mazzanti and F. Nitti, eprint arXiv:0804.0899.
- [37] S. S. Gubser, A. Nellore, S. S. Pufu and F. D. Rocha, e-Print: arXiv:0804.1950 .
- [38] A. Cherman, T. D. Cohen and E. S. Werbos, e-Print: arXiv:0804.1096.
- [39] N. Evans and E. Threlfall, e-Print: arXiv:0805.0956.